IEEE Access
Multidisciplinary | Rapid Review | Open Access Journal

Received January 4, 2021, accepted January 21, 2021, date of publication January 25, 2021, date of current version February 1, 2021.

Digital Object Identifier 10.1109/ACCESS.2021.3054361

m6A-NeuralTool: Convolution Neural Tool for RNA N6-Methyladenosine Site Identification in Different Species

MOBEEN UR REHMAN[1,2], KIM JEE HONG[3], HILAL TAYARA[4], AND KIL TO CHONG[1,5], (Member, IEEE)

[1]Department of Electronics and Information Engineering, Jeonbuk National University, Jeonju 54896, South Korea
[2]Department of Avionics Engineering, Air University, Islamabad 44000, Pakistan
[3]Department of New & Renewable Energy, VISION College of Jeonju, Jeonju 55069, South Korea
[4]School of International Engineering and Science, Jeonbuk National University, Jeonju 54896, South Korea
[5]Advanced Electronics and Information Research Center, Jeonbuk National University, Jeonju 54896, South Korea

Corresponding author: Hilal Tayara (hilaltayara@jbnu.ac.kr) and Kil To Chong (kitchong@jbnu.ac.kr)

This work was supported in part by the National Research Foundation of Korea (NRF) through the Ministry of Science and ICT (MSIT), Korean Government under Grant 2020R1A2C2005612, in part by the National Research Foundation (NRF) funded by the Ministry of Science and ICT (MSIT), Korean Government through the Brain Research Program under Grant NRF-2017M3C7A1044816, and in part by research funds for newly appointed professors of Jeonbuk National University in 2020.

ABSTRACT An important role is played by N6-methyladenosine (m6A) in RNA methylation modification. The modification information is crucially required for development in the field of medicine. Biochemical experiments for m6A identification have demonstrated high-quality results. However, this process is not a feasible solution due to its cost and time constraints. Recently, artificial intelligence has played a role to produce effective models which can be utilized for speedy and efficient identification of N6-methyladenosine sites. In consensus, a computational model named as m6A-NeuralTool is proposed in this study. The m6A-NeuralTool makes the final prediction for the identification of m6A sites by applying majority voting on three different sub-architectures. These sub-architectures uses a set of Convolution layers to extract the important features from the one-hot encoded input sequence. Further, one of the sub-architectures uses fully connected layers for the classification while the other two uses Support Vector Machine and Naive Bayes. The proposed m6A-NeuralTool is evaluated on four different species datasets using 10-fold cross-validation, where the proposed tool outperformed the existing state-of-art models for modification identification of m6A sites. When compared with existing models the proposed model increased the accuracy by 14.8%, 8.8%, 6.3%, and 4.9% for the datasets of Saccharomyces cerevisiae (*S. cerevisiae*), Arabidopsis thaliana (*A. thaliana*), Mus musculus (*M. musculus*) and Homo sapiens (*H. sapiens*) species respectively. The proposed model will allow the researchers from the field of bioinformatics and medicine to accurately identify the modification in m6A sites and use the information in the development of different products which would be beneficial for the community. The m6A-NeuralTool can be accessed freely at: http://nsclbio.jbnu.ac.kr/tools/m6A-NeuralTool/

INDEX TERMS RNA N6-methyladenosine, convolution neural network (CNN), support vector machine (SVM), naive bayes (NB), computational biology.

I. INTRODUCTION

The RNA post-transcriptional modification (PTM) is a common phenomenon of biological process. There are more than 160 RNA modifications among which Methyladenosine (m6A) takes place most frequently. The N6-Methyladenosine modification holds a significant role in majority of the cell cycles like cell growth [1], cell progression [2], affecting translation performance [3] and others. Recent studies have suggested that m6A is closely involved in different diseases, such as prostate cancer [4], acute myeloid leukemia [5], thyroid tumour [6], etc. Although our familiarity with the behaviour of methyladenosine is unintelligible, however, to increase the knowledge on the functionality of m6A, it is important to identify its position in transcriptomes.

The associate editor coordinating the review of this manuscript and approving it for publication was Nuno Garcia.

N6-Methyladenosine sites can be identified using two different ways. Firstly there are multiple experiments, such as m6A sequencing (m6A-seq) [7], crosslinking immunoprecipitation [8], Methylated RNA Immunoprecipitation (MeRIP) [9], etc. These utilized experimental techniques have an important role in the identification of m6A sites. But unfortunately, these experimental techniques are not practicable as they are expensive and time-consuming [10]. Therefore, in recent times a new crucial way is explored where computational biology is adopted to identify the modification in methyladenosine.

Machine learning and handcrafted features have contributed greatly in different complicated research problems like image quality assessment [11], [12], human activity classification [13] and medical diagnostic systems [14], [15]. Similarly, in literature research can be found where handcrafted features and machine learning algorithms are adopted for m6A identification task. Dao *et al.* in [16] has proposed a tool named as IRNA-m6A that uses SVM for prediction of m6A modification. Chen *et al.* proposed another algorithm MethyRNA that utilizes nucleotide frequency with SVM for methyladenosine modification identification in *H. sapiens* and *M. musculus* [17]. iMethyl-STTNC was proposed in [18] where split-tetra-nucleotide composition as feature vector and SVM as the classifier is adopted for prediction of m6A. M6AMRFS [19] is another tool in literature which uses dinucleotide binary encoding scheme along with eXtreme Gradient Boosting technique for classification of m6A and non-m6A sequences. The eXtreme Gradient Boosting technique is also used in iMRM with nucleotide chemical properties (NCP) to classify N6-Methyladenosine [20]. The aforementioned models have undoubtedly improved the performance of identifying m6A sites but still, a great potential for improvement is available.

In literature, handcrafted features for modification identification are limited due to bounded knowledge of humans regarding m6A modification. Therefore moving towards deep learning-based models is a viable choice as they have the ability to extract efficient features with human involvement. These features can lead to a robust and efficient model for N6-Methyladenosine site prediction. Deep learning-based architectures have shown remarkable performance in medical imaging [21], [22], image segmentation [23], [24] and computational biology [25]–[30]. In past, few deep learning-based models are proposed for m6A modification identification. BERMP is a neural network-based tool which integrates deep learning technique with random forest to get m6A and non-m6A classification [31]. Another model named as iN6-Methyl is proposed by Nazari *et al.* which uses CNN model for the predicting m6A sites [32]. iN6-Methyl extracts the feature using natural language technique known as word2vec. These extracted features are then embedded to a CNN model for the purpose of classification. Some other models like DeepM6ASeq [33], Gene2Vec [34] and iPseU-CNN [35] are also in the list of deep learning-based computational methods for m6A classification. Proposed techniques in literature have produced good results but still, a research gap is available where CNN itself along with the combination of CNN and other machine learning algorithms can be explored.

TABLE 1. Summary of the datasets used in this study. Acronyms: Sequence (Seq), Number (No.), Length(Len.).

Specie	Compiled By	Seq Class	No. of Seq	Seq Len.
S. cerevisiae	Zhu *et al.* [36]	m6A non-m6A	3270 3270	51nt
A. thaliana	Wang*et al.* [37]	m6A non-m6A	2100 2100	101nt
M. musculus	Dan *et al.* [7]	m6A non-m6A	725 725	41nt
H. sapiens	Chen *et al.* [17]	m6A non-m6A	1130 1130	41nt

Being inspired by the success of CNN models for RNA modification identification, the present work proposes a high performing CNN based tool, called m6A-NeuralTool, for identifying m6A sites in different species. The proposed architecture of m6A-NeuralTool uses three sub-architectures for the prediction of modification in N6-Methyladenosine sites. The m6A-NeuralTool predicts the modification based on the decision taken by these sub-architectures. The optimum parameters of sub-architectures are set using hyper-parameter tuning. The proposed architecture is evaluated on RNA sequences of four different species. Performance of m6A-NeuralTool is evaluated using K-fold cross-validation, where the value of K is 10. The proposed model has exhibited a huge increase in performance when compared with the existing state of the art techniques.

II. MATERIALS AND METHODS

This section discusses the benchmark dataset, proposed neural tool for identifying m6A sites in different species and the figure of merit.

A. BENCHMARK DATASET

For this research benchmark datasets of four different species is taken into account. The *S. cerevisiae* genome dataset was compiled by Zhu *et al.* in 2019 [36], this dataset is labeled as M6A6540. *S. cerevisiae* genome dataset contains 3270 m6A RNA sequences and 3270 non-m6A RNA sequences where the length of every sequence is 51nt.In 2018 Wang*et al.* prepared the *A. thaliana* genome dataset which consists of 2100 positive and 2100 negative sequences [37]. The length of each sequence in the dataset is 101nt. The *M. musculus* genome dataset was arranged by Dan *et al.* in 2012 [7]. In the dataset, there are 725 positive RNA methyladenosin site sequences and 725 negative RNA non-methyladenosin site sequences with a length of 41nt. Dataset for *H. sapien* genome was proposed in 2017 by Chen *et al.* The dataset consists of 2260 sequences out of which half are methyladenosine while the remaining half are non-methyladenosine [17]. Each sequence in the dataset is of length 41nt. All sequences from different species are centered

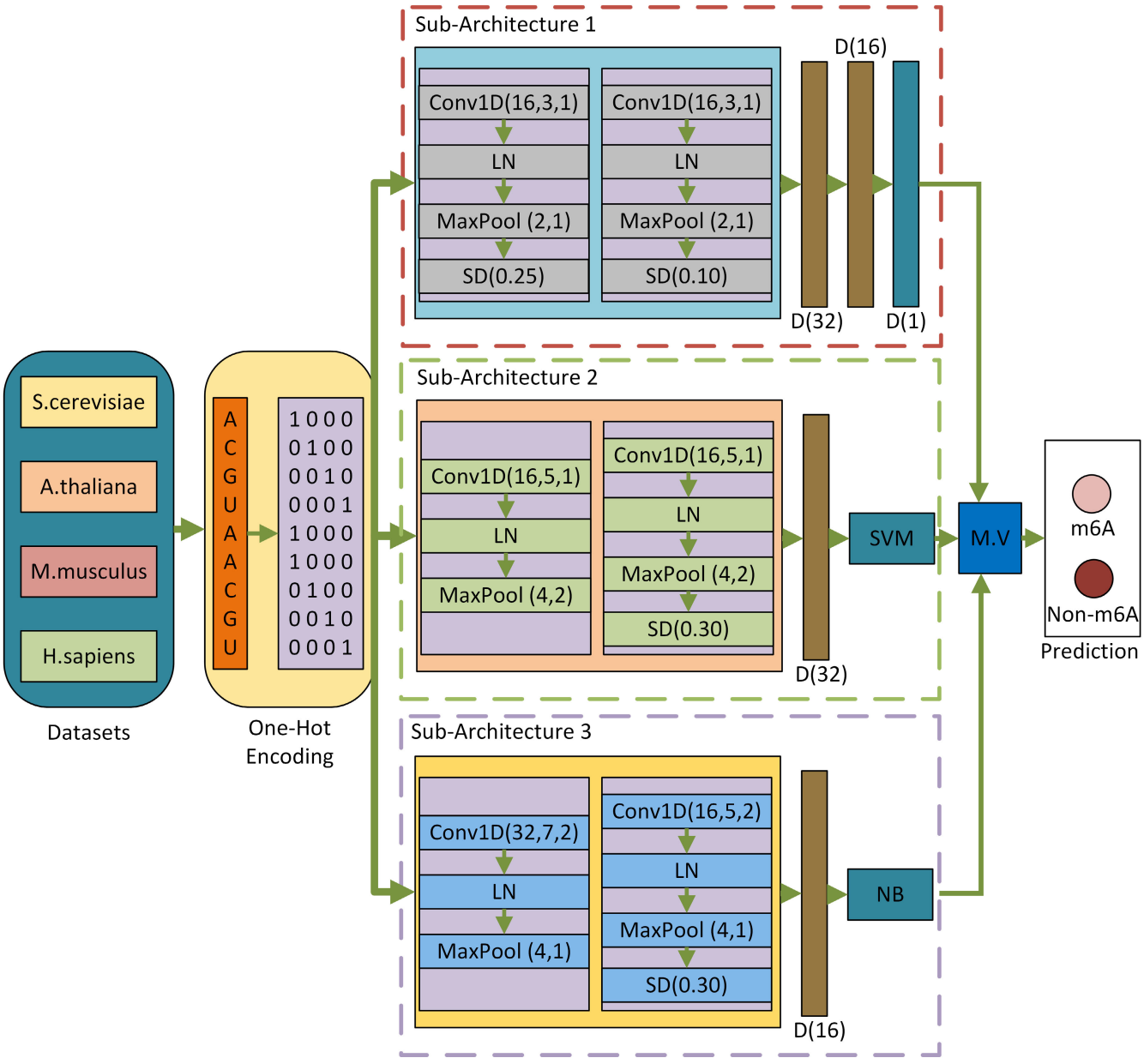

FIGURE 1. Framework of m6A-NeuralTool. Acronyms: Convolution 1 Dimension (Conv1D), Layer Normalization (LN), MaxPool (Max Pooling), Spatial Dropout (SD), Dense (D), Conv1d (number of filters, size of filters, stride length), MaxPool (pool size, stride length), SD (ratio of features discarded), Support Vector Machine (SVM), Naive Bayes (NB), Majority Voting (M.V).

with the m6A and non-m6A sites. Information regarding used datasets is shown in Table 1.

B. PROPOSED ARCHITECTURE

A CNN based tool is proposed for the classification of m6A sites. Proposed architecture (m6A-NeuralTool) comprises of three sub-architecture which contribute towards the final prediction of modification in N6-Methyladenosine as can be seen in figure 1. All three sub-architectures are trained individually. m6A-NeuralTool is competent to automatically learn the effective features from the input RNA sequences. The input of the architecture is RNA sequence with a length of 51nt, 101nt and 41nt depending on the specie. The input RNA sequence is encoded using one-hot encoding where nucleotides A, C, G, U are represented as follows,

$$A \rightarrow (1, 0, 0, 0)$$
$$C \rightarrow (0, 1, 0, 0)$$
$$G \rightarrow (0, 0, 1, 0)$$
$$U \rightarrow (0, 0, 0, 1)$$

The four-channel encoded vector of RNA sequence is separately given as an input to all three sub-architectures. For all three sub-architectures fine tuning is carried out using the

grid search method. Optimal parameters for the number of convolution filters, convolution filter size, pool size, stride length, dropout ratio and dense layer neurons are selected to get the best performance from every sub-architecture.

Sub-architecture 1 is an end to end neural network with two convolution layers where every convolution layer is followed by layer normalization, max-pooling layer, spatial dropout layer. The convolution layers use 16 filters with a size of 3 and stride length of 1. Max pooling layers have a pool size of 2 and stride length of 1. First spatial dropout layer drops the features with ratio 0.25 while the second spatial dropout layer drops the features with ratio 0.10. The output of second dropout layer is given to the three fully connected layers with 32, 16, 1 neuron for the prediction. The first two dense layers use ReLU activation function while the last dense layer uses sigmoid activation function. The equations for ReLU activation function and sigmoid activation function are as follows,

$$\text{ReLU}(y) = max(0, y) \tag{1}$$

$$\text{Sigmoid}((y) = \frac{1}{1 + exp(-y)} \tag{2}$$

Binary cross-entropy [38] is used as a loss function and adaptive moment estimation (Adam) optimizer [39] is used for model optimization. The numerical representation of binary cross-entropy is shown in equation 3.

$$BCE = \begin{cases} -log(Sigmoid(y)) & \text{if } l_1 = 1 \\ -log(1 - Sigmoid(y)) & \text{if } l_1 = 0 \end{cases} \tag{3}$$

where l_1 is the label of class sample.

Sub-architecture 2 uses CNN model for feature extraction and Support Vector Machine SVM model for classification. CNN model uses two convolution layers, two normalization layers, two max-pooling layers and one spatial dropout layer. Both Convolution layers use 16 different filters of size 5 and stride length 1. While both max-pooling layers have a pool size of 4 and stride length of 2. Spatial dropout layer is applied to the output of second max pooling layer with a dropping ratio of 0.30. The extracted features using the CNN model are flattened and given to the dense layer with 32 neurons. The vector attained from the dense layer is used by SVM for classification. SVM is counted as one of the most efficient statistical learning models for the purpose of classification [40].

Sub-architecture 3 also uses the CNN model for feature extraction while Naive Bayes (NB) as a classifier. CNN model of sub-architecture 3 uses two convolution layers. First convolution layer has 32 filters with the filter size of 7 and stride length of 2, while the second convolution layer has 16 filters of size 5 with stride length 2. Both convolution layers are followed by layer normalization and max pooling. The pool size of 4 and stride length of 1 is used in both max-pooling layers. The second max-pooling layer is followed by a spatial dropout layer where 0.30 ratio of features is dropped out. The optimized feature vector from the CNN model is embedded into the dense layer with 16 neurons which is followed by Naive Bayes classifier. Naive Bayes classifier works under the principle of Bayes theorem, where the maximum probability for the specified class is calculated. For class 'c' the equation followed for classification is as follows,

$$c = argmax_c P(c) \Pi_{j=1}^{n} P(f_j|c) \tag{4}$$

where $P(c)$ is the probability of class 'c', n is the total number of features embedded into Naive Bayes and f is the feature set. In our case value of n is 16.

For all convolution layers in three sub-architecture exponential linear uni ELU activation function is used. The equation of the ELU activation function is,

$$\begin{cases} y & \text{if } y \geq 0 \\ \alpha(exp(y) - 1) & \text{if } y < 0 \end{cases} \tag{5}$$

To prevent all three sub-architectures from overfitting, Ridge Regression (L2 Regularization) method is used in convolution and dense layers.

After taking prediction from all three sub-architectures, m6A-NeuralTool applies the majority voting on three predictions to get the final prediction about the class. In majority voting, the vote goes towards the class which is predicted by at least two sub-architectures.

C. EVALUATION METRICS

For evaluating the performance of m6A-NeuralTool, 10-fold cross-validation is carried out. In this method whole dataset is divided into ten sets where nine sets are used for training purpose while a single set is used to test the model. This process is carried out ten times and every time a new test set is selected while the previous test set returns back to training sets. After completion of this recursive process, an average is taken out for all 10 folds. Existing models for m6A classification uses Sensitivity (SeN), Specificity (SPe), Accuracy (ACC) and Mathew's correlation coefficient (MCC) for performance evaluation. We also have used these four evaluation metrics. The mathematical representation of these metrics are as follows,

$$SeN = \frac{TP}{TP + FN} \tag{6}$$

$$SPe = \frac{TN}{TN + FP} \tag{7}$$

$$ACC = \frac{TP + TN}{TP + TN + FP + FN} \tag{8}$$

$$MCC = \frac{TP \times TN - FP \times FN}{\sqrt{(TP+FP)(TP+FN)(TN+FP)(TN+FN)}} \tag{9}$$

where True Positives (TP), False Positives (FP), True Negatives (TN) and False Negatives (FN) are defined as,

TP = m6A correctly predicted as m6A
FP = Non-m6A incorrectly predicted as m6A
TN = Non-m6A correctly predicted as Non-m6A
FN = m6A incorrectly predicted as Non-m6A

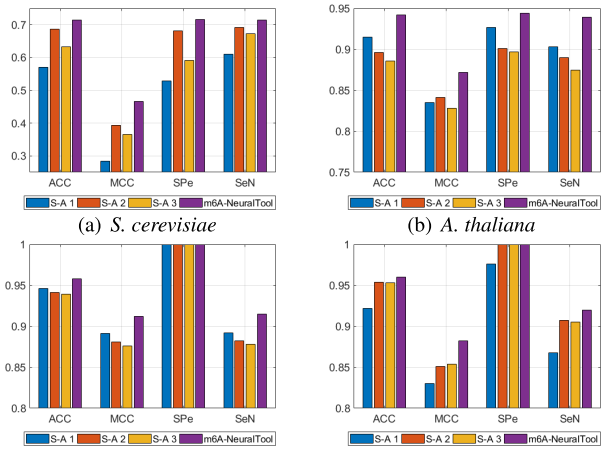

(a) *S. cerevisiae* (b) *A. thaliana* (c) *M. musculus* (d) *H. sapiens*

FIGURE 2. Visual performance comparison between proposed sub-architectures and proposed m6A-NeuralTool.

TABLE 2. Performance comparison of proposed sub-architectures and proposed m6A-NeuralTool (The highest values for evaluation metrics on different species are shown in bold.).

Species	Architecture	SeN	SPe	ACC	MCC
S. cerevisiae	Sub-Architecture 1	0.611	0.528	0.570	0.284
	Sub-Architecture 2	0.692	0.681	0.687	0.393
	Sub-Architecture 3	0.672	0.592	0.632	0.366
	m6A-NeuralTool	**0.715**	**0.716**	**0.715**	**0.466**
A. thaliana	Sub-Architecture 1	0.903	0.927	0.915	0.835
	Sub-Architecture 2	0.890	0.901	0.896	0.841
	Sub-Architecture 3	0.875	0.897	0.886	0.828
	m6A-NeuralTool	**0.939**	**0.944**	**0.942**	**0.872**
M. musculus	Sub-Architecture 1	0.892	1	0.946	0.891
	Sub-Architecture 2	0.882	1	0.941	0.881
	Sub-Architecture 3	0.878	1	0.939	0.876
	m6A-NeuralTool	**0.915**	**1**	**0.958**	**0.912**
H. sapiens	Sub-Architecture 1	0.868	0.976	0.922	0.830
	Sub-Architecture 2	0.907	1	0.954	0.851
	Sub-Architecture 3	0.905	1	0.953	0.854
	m6A-NeuralTool	**0.920**	**1**	**0.960**	**0.882**

III. RESULTS AND DISCUSSION

The m6A-NeuralTool is evaluated on benchmark datasets of four species using 10-fold cross-validation. As discussed earlier m6A-NeuralTool comprises of three sub-architectures. The performance of individual proposed sub-architectures is evaluated along with the proposed model (m6A-NeuralTool) which includes majority voting between proposed sub-architectures for final prediction.

Figure 2 shows the visual performance comparison between individual sub-architectures and m6A-NeuralTool. Further table 2 illustrates the numerical comparison of sub-architectures and m6A-NeuralTool on different species. A significant improvement can be observed when the majority voting on individual sub-architectures is applied. For *S. cerevisiae* and *H. sapiens* sub-architecture 2 represents higher performance than other sub-architectures. While in the case of *M. musculus* and *A. thaliana* the sub-architecture 1 showed better performance than other sub-architectures. But, applying majority voting on different sub-architectures further improves the classification performance on every dataset.

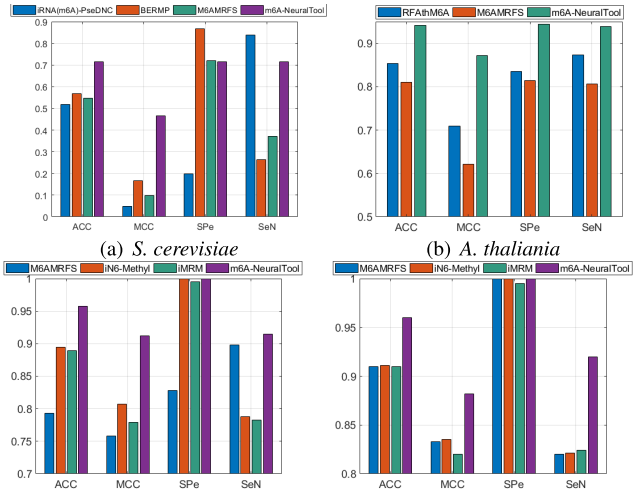

(a) *S. cerevisiae* (b) *A. thaliania* (c) *M. musculus* (d) *H. sapiens*

FIGURE 3. Visual performance comparison between m6A-NeuralTool and state-of-the-art techniques.

TABLE 3. Performance comparison of m6A-NeuralTool with state-of-the-art techniques (The highest values for different evaluation metrics on different species are shown in bold.).

Species	Architecture	SeN	SPe	ACC	MCC
S. cerevisiae	iRNA(m6A)-PseDNC [41]	**0.839**	0.199	0.519	0.049
	BERMP [31]	0.265	**0.868**	0.567	0.167
	M6AMRFS [19]	0.371	0.721	0.546	0.099
	m6A-NeuralTool	0.715	0.716	**0.715**	**0.466**
A. thaliana	RFAthM6A [37]	0.873	0.835	0.854	0.709
	M6AMRFS [19]	0.806	0.814	0.810	0.621
	m6A-NeuralTool	**0.939**	**0.944**	**0.942**	**0.872**
M. musculus	M6AMRFS [19]	0.898	0.828	0.793	0.758
	iN6-Methyl [32]	0.788	1	0.895	0.807
	iMRM [20]	0.783	0.995	0.889	0.779
	m6A-NeuralTool	**0.915**	**1**	**0.958**	**0.912**
H. sapiens	M6AMRFS [19]	0.82	1	0.91	0.833
	iN6-Methyl [32]	0.821	1	0.911	0.835
	iMRM [20]	0.824	0.995	0.91	0.82
	m6A-NeuralTool	**0.920**	**1**	**0.960**	**0.882**

Figure 3 gives the visual representation of the comparison between m6A-NeuralTool and state-of-the-art techniques for different species. Further table 3 exhibits the numerical comparison of state-of-the-art tools with m6A-NeuralTool for m6A modification identification. The m6A-NeuralTool outperformed in all species. High performance by m6A-NeuralTool can be seen for every figure of merit in case of *A. thaliana*, *M. musculus* and *H. sapiens*. For *S. cerevisiae* benchmark dataset the proposed model showed improvement in terms of ACC and MCC, while in terms of SeN iRNA(m6A)-PseDNC have achieved better results. Unfortunately, iRNA(m6A)-PseDNC showed really poor performance in SPe. BEMRP have attained highest SPe for *S. cerevisiae* specie but the model was unable to deliver high SeN. For *S. cerevisiae*, m6A-NeuralTool demonstrates a balanced performance for SPe and SeN, which results in higher ACC and MCC.

The Matthews correlation coefficient (MCC) represents the quality of binary classification model. The m6A-NeuralTool have depicted improvement in MCC by

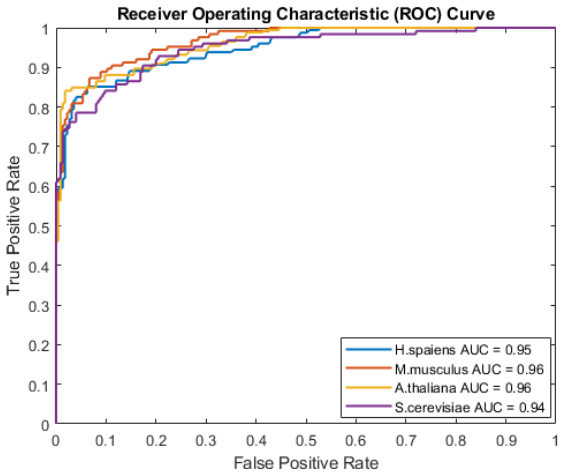

FIGURE 4. The auROC curves of the proposed model for different species.

TABLE 4. Performance comparison of m6A-NeuralTool with state-of-the-art techniques on M6A2614 dataset of *S. cerevisiae* species (The highest values for different evaluation metrics are shown in bold.).

Architecture	SeN	SPe	ACC	MCC
M6AMRFS [19]	0.752	0.733	0.743	0.485
iN6-Methyl [32]	0.762	0.746	0.754	0.508
m6A-NeuralTool	**0.783**	**0.796**	**0.790**	**0.614**

29.9%, 16.3%, 10.5%, 4.7% for *S. cerevisiae*, *A. thaliana*, *M. musculus* and *H. sapiens* respectively. This enhancement by m6A-NeuralTool in the MCC replicates its high quality. Figure 4 illustrates the Receiver Operating Characteristic (ROC) curve achieved by m6A-NeuralTool, for different species. The m6A-NeuralTool have attained an Area Under the ROC Curve (AUC) of 0.95, 0.96, 0.96, 0.94 for benchmark dataset of *H. sapiens*, *M. musculus*, *A. thaliana*, *S. cerevisiae* respectively.

The generalization of any model is important. For this purpose researchers were able to find another dataset of *S. cerevisiae* (named as 'M6A2614') [42], which is used as an independent dataset to study the generalization of m6A-NeuralTool. In total there are 2614 sequences in M6A2614 dataset out of which 1307 are negative and 1307 are positive. We trained the model on M6A6540 dataset of *S. cerevisiae* (benchmark dataset) and tested it on M6A2614 independent dataset of *S. cerevisiae*. The achieved results by m6A-Neural tool are compared with the state-of-the-art models for M6A2614 dataset, shown in table 4. Even in this case, m6A-NeuralTool has shown an improvement when compared with state-of-the-art techniques. Here it is important to keep in mind that M6A2614 dataset is treated as an independent dataset for m6A-NeuralTool.

The modeling of RNA motifs with insertion/deletion (indels) plays an important role in functional genomics. The prediction model should be efficient enough to effectively model the RNA motifs. In this regard to access the quality of m6A-NeuralTool, a test is carried out using silico mutagenesis method. As per silico mutagenesis method, the nucleotides

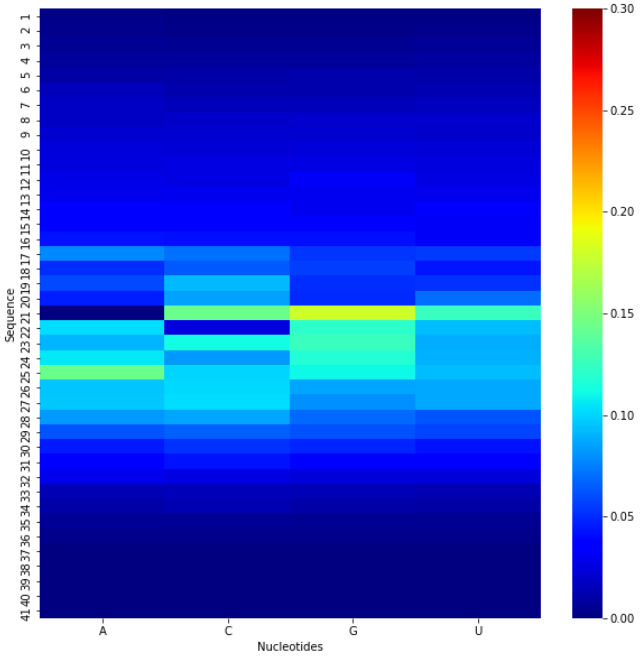

FIGURE 5. Heat Map to study the effect of mutation on m6A-NeuralTool model prediction.

in the sequences of the dataset are mutated computationally to study its effect on model prediction. In this test, the sequences with length 41nt are taken into consideration. One after another all nucleotides at every position of the sequence are mutated. The absolute difference between the predictions of the original sequence and mutated sequences is computed and stored. Averaged predicted score for all mutations is calculated over all the sequences. Lastly, the averaged predicted score is used to construct the heat map, shown in figure 5. As illustrated in the heat map, the prediction by m6A-NeuralTool is affected higher for the mutations occurred at the center of the sequence rather than at starting and ending nucleotides of the sequence.

IV. CONCLUSION

N6-Methyladenosine modification identification is the important information required to investigate different biological functions. In this study, authors have proposed a computational tool named as m6A-NeuralTool. The m6A-NeuralTool can effectively identify RNA-m6A modification using multiple sub-architectures. The proposed model consists of three sub-architectures which individually perform classification and majority voting is applied to get the final prediction. All three sub-architectures uses different CNN models for feature extraction. For classification, the three sub-architectures uses, unlike learning machines which are fully connected layers, Support Vector Machine and Naive Bayes. The m6A-NeuralTool is evaluated on four different species using 10 fold cross-validation. Proposed model has shown great improvement for all the species dataset when compared with existing state-of-the-art

techniques. The goal to establish m6A-NeuralTool is to employ it for distinct research fields operational in the development of medicine and bioinformatics. For this reason, free access to a web server is publicly made available at: http://nsclbio.jbnu.ac.kr/tools/m6A-NeuralTool/

ACKNOWLEDGMENT

(Mobeen Ur Rehman and Kim Jee Hoong contributed equally to this work.)

REFERENCES

[1] J. A. Bokar, "The biosynthesis and functional roles of methylated nucleosides in eukaryotic mRNA," in *Fine-Tuning RNA Functions By Modification Editing*. Cham, Switzerland: Springer, 2005, pp. 141–177.

[2] Y. Wang, Y. Li, J. I. Toth, M. D. Petroski, Z. Zhang, and J. C. Zhao, "N6-methyladenosine modification destabilizes developmental regulators in embryonic stem cells," *Nature Cell Biol.*, vol. 16, no. 2, pp. 191–198, Feb. 2014.

[3] X. Wang, B. S. Zhao, I. A. Roundtree, Z. Lu, D. Han, H. Ma, X. Weng, K. Chen, H. Shi, and C. He, "N6-methyladenosine modulates messenger RNA translation efficiency," *Cell*, vol. 161, no. 6, pp. 1388–1399, Jun. 2015.

[4] M. J. Machiela *et al.*, "Association of type 2 diabetes susceptibility variants with advanced prostate cancer risk in the breast and prostate cancer cohort consortium," *Amer. J. Epidemiol.*, vol. 176, no. 12, pp. 1121–1129, Dec. 2012.

[5] H. Bansal, Q. Yihua, S. P. Iyer, S. Ganapathy, D. Proia, L. O. Penalva, P. J. Uren, U. Suresh, J. S. Carew, A. B. Karnad, S. Weitman, G. E. Tomlinson, M. K. Rao, S. M. Kornblau, and S. Bansal, "WTAP is a novel oncogenic protein in acute myeloid leukemia," *Leukemia*, vol. 28, no. 5, pp. 1171–1174, May 2014.

[6] K.-J. Heiliger, J. Hess, D. Vitagliano, P. Salerno, H. Braselmann, G. Salvatore, C. Ugolini, I. Summerer, T. Bogdanova, K. Unger, G. Thomas, M. Santoro, and H. Zitzelsberger, "Novel candidate genes of thyroid tumourigenesis identified in Trk-T1 transgenic mice," *Endocrine Rel. Cancer*, vol. 19, no. 3, p. 409, 2012.

[7] D. Dominissini, S. Moshitch-Moshkovitz, S. Schwartz, M. Salmon-Divon, L. Ungar, S. Osenberg, K. Cesarkas, J. Jacob-Hirsch, N. Amariglio, M. Kupiec, R. Sorek, and G. Rechavi, "Topology of the human and mouse m^6A RNA methylomes revealed by m^6A-seq," *Nature*, vol. 485, no. 7397, pp. 201–206, 2012.

[8] S. Ke, E. A. Alemu, C. Mertens, E. C. Gantman, J. J. Fak, A. Mele, B. Haripal, I. Zucker-Scharff, M. J. Moore, C. Y. Park, C. B. Vågbø, A. Kuśnierczyk, A. Klungland, J. E. Darnell, and R. B. Darnell, "A majority of m^6A residues are in the last exons, allowing the potential for 3′ UTR regulation," *Genes Develop.*, vol. 29, no. 19, pp. 2037–2053, Oct. 2015.

[9] K. D. Meyer, Y. Saletore, P. Zumbo, O. Elemento, C. E. Mason, and S. R. Jaffrey, "Comprehensive analysis of mRNA methylation reveals enrichment in 3 UTRS and near stop codons," *Cell*, vol. 149, no. 7, pp. 1635–1646, 2012.

[10] Z. Chen, P. Zhao, F. Li, Y. Wang, A. I. Smith, G. I. Webb, T. Akutsu, A. Baggag, H. Bensmail, and J. Song, "Comprehensive review and assessment of computational methods for predicting RNA post-transcriptional modification sites from RNA sequences," *Briefings Bioinf.*, vol. 21, no. 5, pp. 1676–1696, Sep. 2020.

[11] I. F. Nizami, M. Majid, M. ur Rehman, S. M. Anwar, A. Nasim, and K. Khurshid, "No-reference image quality assessment using bag-of-features with feature selection," *Multimedia Tools Appl.*, vol. 79, no. 11, pp. 7811–7836, 2020.

[12] I. F. Nizami, M. ur Rehman, M. Majid, and S. M. Anwar, "Natural scene statistics model independent no-reference image quality assessment using patch based discrete cosine transform," *Multimedia Tools Appl.*, vol. 79, no. 35, pp. 26285–26304, 2020.

[13] M. Batool, A. Jalal, and K. Kim, "Telemonitoring of daily activity using accelerometer and gyroscope in smart home environments," *J. Electr. Eng. Technol.*, vol. 15, no. 6, pp. 2801–2809, 2020.

[14] M. Ur Rehman, Z. Abbas, S. H. Khan, S. H. Ghani, and S. Najam, "Diabetic retinopathy fundus image classification using discrete wavelet transform," in *Proc. 2nd Int. Conf. Eng. Innov. (ICEI)*, Jul. 2018, pp. 75–80.

[15] Z. Abbas, M.-U. Rehman, S. Najam, and S. M. Danish Rizvi, "An efficient gray-level co-occurrence matrix (GLCM) based approach towards classification of skin lesion," in *Proc. Amity Int. Conf. Artif. Intell. (AICAI)*, Feb. 2019, pp. 317–320.

[16] F.-Y. Dao, H. Lv, Y.-H. Yang, H. Zulfiqar, H. Gao, and H. Lin, "Computational identification of N6-methyladenosine sites in multiple tissues of mammals," *Comput. Struct. Biotechnol. J.*, vol. 18, pp. 1084–1091, Jan. 2020.

[17] W. Chen, H. Tang, and H. Lin, "MethyRNA: A Web server for identification of N6-methyladenosine sites," *J. Biomol. Struct. Dyn.*, vol. 35, no. 3, pp. 683–687, Feb. 2017.

[18] S. Akbar and M. Hayat, "IMethyl-STTNC: Identification of N6-methyladenosine sites by extending the idea of SAAC into Chou's PseAAC to formulate RNA sequences," *J. Theor. Biol.*, vol. 455, pp. 205–211, Oct. 2018.

[19] X. Qiang, H. Chen, X. Ye, R. Su, and L. Wei, "M6AMRFS: Robust prediction of N6-methyladenosine sites with sequence-based features in multiple species," *Frontiers Genet.*, vol. 9, p. 495, Oct. 2018.

[20] K. Liu and W. Chen, "IMRM: A platform for simultaneously identifying multiple kinds of RNA modifications," *Bioinformatics*, vol. 36, no. 11, pp. 3336–3342, Jun. 2020.

[21] M. U. R. Rehman, S. H. Khan, Z. Abbas, and S. M. D. Rizvi, "Classification of diabetic retinopathy images based on customised CNN architecture," in *Proc. Amity Int. Conf. Artif. Intell. (AICAI)*, Feb. 2019, pp. 244–248.

[22] M. U. R. Rehman, S. H. Khan, S. M. D. Rizvi, Z. Abbas, and A. Zafar, "Classification of skin lesion by interference of segmentation and convolotion neural network," in *Proc. 2nd Int. Conf. Eng. Innov. (ICEI)*, Jul. 2018, pp. 81–85.

[23] T. Ilyas, A. Khan, M. Umraiz, and H. Kim, "SEEK: A framework of superpixel learning with CNN features for unsupervised segmentation," *Electronics*, vol. 9, no. 3, p. 383, Feb. 2020.

[24] A. Khan, T. Ilyas, M. Umraiz, Z. I. Mannan, and H. Kim, "CED-net: Crops and weeds segmentation for smart farming using a small cascaded encoder-decoder architecture," *Electronics*, vol. 9, no. 10, p. 1602, Oct. 2020.

[25] A. Wahab, S. D. Ali, H. Tayara, and K. To Chong, "IIM-CNN: Intelligent identifier of 6 mA sites on different species by using convolution neural network," *IEEE Access*, vol. 7, pp. 178577–178583, 2019.

[26] O. Mahmoudi, A. Wahab, and K. T. Chong, "IMethyl-deep: N6 methyladenosine identification of yeast genome with automatic feature extraction technique by using deep learning algorithm," *Genes*, vol. 11, no. 5, p. 529, May 2020.

[27] W. Alam, S. D. Ali, H. Tayara, and K. T. Chong, "A CNN-based RNA N6-methyladenosine site predictor for multiple species using heterogeneous features representation," *IEEE Access*, vol. 8, pp. 138203–138209, 2020.

[28] A. Wahab, O. Mahmoudi, J. Kim, and K. T. Chong, "DNC4mC-deep: Identification and analysis of DNA N4-methylcytosine sites based on different encoding schemes by using deep learning," *Cells*, vol. 9, no. 8, p. 1756, Jul. 2020.

[29] M. U. Rehman and K. T. Chong, "DNA6 mA-MINT: DNA-6 mA modification identification neural tool," *Genes*, vol. 11, no. 8, p. 898, Aug. 2020.

[30] S. Park, A. Wahab, I. Nazari, J. H. Ryu, and K. T. Chong, "I6 mA-DNC: Prediction of DNA N6-methyladenosine sites in rice genome based on dinucleotide representation using deep learning," *Chemometric Intell. Lab. Syst.*, vol. 204, Sep. 2020, Art. no. 104102.

[31] Y. Huang, N. He, Y. Chen, Z. Chen, and L. Li, "BERMP: A cross-species classifier for predicting m^6A sites by integrating a deep learning algorithm and a random forest approach," *Int. J. Biol. Sci.*, vol. 14, no. 12, p. 1669, 2018.

[32] I. Nazari, M. Tahir, H. Tayara, and K. T. Chong, "IN6-methyl (5-step): Identifying RNA N6-methyladenosine sites using deep learning mode via Chou's 5-step rules and Chou's general PseKNC," *Chemometric Intell. Lab. Syst.*, vol. 193, Oct. 2019, Art. no. 103811.

[33] Y. Zhang and M. Hamada, "DeepM6ASeq: Prediction and characterization of m6A-containing sequences using deep learning," *BMC Bioinf.*, vol. 19, no. S19, p. 524, Dec. 2018.

[34] Q. Zou, P. Xing, L. Wei, and B. Liu, "Gene2Vec: Gene subsequence embedding for prediction of mammalian N6-methyladenosine sites from mRNA," *RNA*, vol. 25, no. 2, pp. 205–218, Feb. 2019.

[35] M. Tahir, H. Tayara, and K. T. Chong, "IPSEU-CNN: Identifying RNA pseudouridine sites using convolutional neural networks," *Mol. Therapy-Nucleic Acids*, vol. 16, pp. 463–470, 2019.

[36] X. Zhu, J. He, S. Zhao, W. Tao, Y. Xiong, and S. Bi, "A comprehensive comparison and analysis of computational predictors for RNA N6-methyladenosine sites of saccharomyces cerevisiae," *Briefings Funct. Genomics*, vol. 18, no. 6, pp. 367–376, 2019.
[37] X. Wang and R. Yan, "RFAthM6A: A new tool for predicting m6A sites in Arabidopsis thaliana," *Plant Mol. Biol.*, vol. 96, no. 3, pp. 327–337, Feb. 2018.
[38] P.-T. de Boer, D. P. Kroese, S. Mannor, and R. Y. Rubinstein, "A tutorial on the cross-entropy method," *Ann. Oper. Res.*, vol. 134, no. 1, pp. 19–67, Feb. 2005.
[39] D. P. Kingma and J. Ba, "Adam: A method for stochastic optimization," 2014, *arXiv:1412.6980*. [Online]. Available: http://arxiv.org/abs/1412.6980
[40] V. Vapnik, *The Nature of Statistical Learning Theory*. Cham, Switzerland: Springer, 2013.
[41] W. Chen, H. Ding, X. Zhou, H. Lin, and K.-C. Chou, "IRNA(m6A)-PseDNC: Identifying N6-methyladenosine sites using pseudo dinucleotide composition," *Anal. Biochem.*, vols. 561–562, pp. 59–65, Nov. 2018.
[42] S. Schwartz, S. D. Agarwala, M. R. Mumbach, M. Jovanovic, P. Mertins, A. Shishkin, Y. Tabach, T. S. Mikkelsen, R. Satija, G. Ruvkun, S. A. Carr, E. S. Lander, G. R. Fink, and A. Regev, "High-resolution mapping reveals a conserved, widespread, dynamic mRNA methylation program in yeast meiosis," *Cell*, vol. 155, no. 6, pp. 1409–1421, Dec. 2013.

MOBEEN UR REHMAN received the B.Sc. degree in electrical engineering from Bahria University, Islamabad, Pakistan, in 2017, and the M.Sc. degree (Hons.) in avionics engineering from Air University, Islamabad, in 2019. For several years, he served as a Research Associate with the CSES, Institute of Avionics and Aeronautics, Air University. He is currently serving as a Research Scholar with Jeonbuk National University, Jeonju, South Korea. His research interests include artificial intelligence, medical imaging, computational intelligence, bioinformatics, and pattern recognition.

KIM JEE HONG received the Ph.D. degree in control and measurement engineering from Chonbuk National University, in 2010. He is currently a Professor with the Department of New and Renewable Energy, VISION College of Jeonju, South Korea, and a member of the Advanced Information and Electronics Research Center, Jeonbuk National University. His research interests include the areas of bioinformatics, artificial intelligence, drug discovery, and big-data in the renewable energy sector.

HILAL TAYARA received the B.Sc. degree in computer engineering from Aleppo University, Aleppo, Syria, in 2008, and the M.S. and Ph.D. degrees in electronics and information engineering from Jeonbuk National University, Jeonju, South Korea, in 2015 and 2019, respectively. He served as a Researcher with Jeonbuk National University. He is currently serving as an Assistant Professor with the School of International Engineering and Science, Jeonbuk National University. His research interests include bioinformatics, machine learning, and image processing.

KIL TO CHONG (Member, IEEE) received the Ph.D. degree in mechanical engineering from Texas A&M University, in 1993. He is currently a Professor with the School of Electronics and Information Engineering, Jeonbuk National University, Jeonju, South Korea. He is the Head of the Advanced Information and Electronics Research Center, Jeonbuk National University, and he is the President of the Korean Electronics Engineering Society, Systems and Control. His research interests include bioinformatics, artificial intelligence, brain disease, and new drug discovery.